Epidermal Growth Factor-mediated Activation of the ETS Domain Transcription Factor Elk-1 Requires Nuclear Calcium*

Thomas Pusl‡§, Julie J. Wu¶, Tracy L. Zimmerman‖, Lei Zhang¶, Barbara E. Ehrlich¶, Martin W. Berchtold, Joannes B. Hoek‡‡, Saul J. Karpen‖, Michael H. Nathanson‡, and Anton M. Bennett§ §§**

*From the ‡Department of Medicine, Yale University School of Medicine, New Haven, Connecticut 06520, the ¶Department of Pharmacology, Yale University School of Medicine, New Haven, Connecticut 06520, the ‖Department of Pediatrics, Baylor College of Medicine, Houston, Texas 77030, the **Department of Molecular Cell Biology, University of Copenhagen, 1353 Copenhagen, Denmark, and the ‡‡Department of Pathology, Anatomy and Cell Biology, Thomas Jefferson University, Philadelphia, Pennsylvania 19107*

Cytosolic and nuclear Ca^{2+} have been shown to differentially regulate transcription. However, the impact of spatially distinct Ca^{2+} signals on mitogen-activated protein kinase-mediated gene expression remains unknown. Here we investigated the role of nuclear and cytosolic Ca^{2+} signals in epidermal growth factor (EGF)-induced transactivation of the ternary complex factor Elk-1 using a GAL4-Elk-1 construct. EGF increased Ca^{2+} in both the nucleus and cytosol of HepG2 or 293 cells. Pretreatment with the intracellular Ca^{2+} chelator bis(2-aminophenyl)ethyleneglycol-*N,N,N′,N′*-tetraacetic acid significantly reduced EGF-induced transactivation of Elk-1, indicating that EGF-stimulated Elk-1 transcriptional activity is dependent on intracellular Ca^{2+}. To determine the relative contribution of nuclear and cytosolic Ca^{2+} signals during EGF-mediated Elk-1 transactivation, Ca^{2+} signals in either compartment were selectively impaired by targeted expression of the Ca^{2+}-binding protein parvalbumin to either the nucleus or cytosol. Suppression of nuclear but not cytosolic Ca^{2+} signals inhibited EGF-induced transactivation of Elk-1. However, suppression of nuclear Ca^{2+} signals did not affect the ability of ERK either to become phosphorylated or to undergo translocation to the nucleus in response to EGF. Elk-1 phosphorylation and nuclear localization following EGF stimulation were also unaffected by suppressing nuclear Ca^{2+} signals. These results suggest that nuclear Ca^{2+} is required for EGF-mediated transcriptional activation of Elk-1 and that phosphorylation of Elk-1 alone is not sufficient to induce its transcriptional activation in response to EGF. Thus, subcellular targeting of parvalbumin reveals a distinct role for nuclear Ca^{2+} signals in mitogen-activated protein kinase-mediated gene transcription.

Ca^{2+} is a fundamental second messenger that mediates a range of biological processes, including fertilization, mitogenesis, exocytosis, synaptic plasticity, gene expression, differentiation, proliferation, and apoptosis (1–9). Although it is not completely established how Ca^{2+} coordinates such diverse effects, both the amplitude and frequency of Ca^{2+} signals have been shown to contribute to its specificity (10–12). Further specificity of Ca^{2+} signaling is achieved through differences in signaling in discrete subcellular compartments (9, 13–15). For example, separate machinery may be involved for regulating nuclear Ca^{2+} (Ca^{2+}_{nuc})[1] and cytosolic Ca^{2+} (Ca^{2+}_{cyt}) (16–20). Moreover, Ca^{2+}_{nuc} is required for transcription via the cAMP response element (21) and regulation of cAMP response element-binding protein-binding protein activity (22), whereas Ca^{2+}_{cyt} activates transcription through the serum response element (21). Thus, spatially distinct Ca^{2+} signals have distinct cellular effects.

Although our understanding of the distinct roles of both Ca^{2+}_{cyt} and Ca^{2+}_{nuc} in gene expression is limited, it is well established that protein phosphorylation in the nucleus by the mitogen-activated protein kinases (MAPK) is critical for gene regulation (23, 24). Following phosphorylation by the MAPK kinases (MKKs), the extracellular signal-regulated kinases 1 and 2 (ERKs), c-Jun amino-terminal kinases, and p38 MAPKs each translocate to the nucleus (25) where they transactivate various transcription factors by serine and threonine phosphorylation (23, 24). Subsequently, these transcription factors direct transcriptional activation of genes that are essential for the initiation of numerous physiological responses such as mitogenesis, differentiation, and apoptosis (26–29). For example, epidermal growth factor (EGF) receptor stimulation results in nuclear accumulation of activated ERK, where it binds to and phosphorylates the ETS domain-containing transcription factor Elk-1 (23, 30, 31). Phosphorylation of Elk-1 is thought to increase its transcriptional activity, leading to the transcription of growth-related proteins, most notably c-Fos (32, 33). In addition to ERK activation, EGF and other growth factors raise intracellular free Ca^{2+} levels by activating phospholipase Cγ with subsequent formation of inositol 1,4,5-trisphosphate (34–36). Ca^{2+} modulates several signaling pathways that converge at various points to regulate Elk-1 transcriptional activity. Work from several groups demonstrates that growth factor- and cytokine-induced increases in Ca^{2+} contribute to the acti-

[1] The abbreviations used are: Ca^{2+}_{nuc}, nuclear free calcium; Ca^{2+}_{cyt}, cytosolic free calcium; MAPK, mitogen-activated protein kinase; MKK, MAPK kinase; EGF, epidermal growth factor; ERK, extracellular regulated kinase; PV, parvalbumin; NES, nuclear exclusion signal; NLS, nuclear localization signal; GFP, green fluorescent protein; AM, acetoxymethyl; HA, hemagglutinin; BAPTA, bis(2-aminophenyl)ethyleneglycol-*N,N,N′,N′*-tetraacetic acid.

vation of the ERK/Elk-1 pathway via mechanisms that involve activation of signaling components such as the Src-like kinases, Pyk2, and the Ca^{2+}-sensitive Ras guanine nucleotide-releasing factor (37–39). In addition, growth factor-induced Ca^{2+} increases lead to activation of other pathways such as the Ca^{2+}/calmodulin-dependent protein kinases that also participate in the regulation of Elk-1 (40–43). In contrast to the positive signaling role of Ca^{2+} in growth factor-mediated Elk-1 activation, Ca^{2+} has been proposed to play also a negative role in Elk-1 regulation by growth factors. Following stimulation the ERK, c-Jun amino-terminal kinase, or p38 MAPK activation of Elk-1 is inhibited by the phosphatase calcineurin (44, 45). Thus, growth factor-mediated changes in Ca^{2+} can lead to the regulation of Elk-1 via multiple pathways in both positive and negative manners. The distinct actions of Ca^{2+} when localized to either the nucleus or cytosol might provide some explanation for the complexity of Elk-1 regulation in growth factor signal transduction.

In this study we have investigated the relative contribution of both Ca_{cyt}^{2+} and Ca_{nuc}^{2+} to the regulation of MAPK-mediated gene expression in response to stimulation with EGF by selective targeting of the Ca^{2+} chelator protein parvalbumin (PV) to either the cytosol or the nucleus. Using this novel approach, we have demonstrated that Ca_{nuc}^{2+} but not Ca_{cyt}^{2+} is required for Elk-1 transcriptional activation in response to EGF stimulation.

EXPERIMENTAL PROCEDURES

Cells and Cell Culture—HepG2, SK-HEP-1, 293, and COS cell lines were cultured at 37 °C in 5% CO_2 in Dulbecco's modified Eagle's medium (Invitrogen) containing 10% fetal bovine serum (Sigma), 1 mM sodium pyruvate (Invitrogen), 50 units/ml penicillin (Sigma), and 50 μg/ml streptomycin (Sigma).

Generation of Targeted Parvalbumin Expression Constructs—The nuclearly targeted PV expression vector was constructed by subcloning a *Sal*I/*Not*I fragment representing the full-length rat PV cDNA in-frame into the pCMV-Myc-Nuc vector (Invitrogen). This construct resulted in an in-frame fusion of PV with a Myc epitope and a triplet sequence representing the nuclear localization sequence derived from SV40 and was designated pCMV-PV-Myc-Nuc. To generate a GFP fusion of pCMV-PV-Myc-Nuc, the GFP coding sequence was PCR-amplified from pCMV-Myc-Cyto-GFP (Invitrogen) using the primers 5′-AT AAG AAT GCG GCC GCA ATG GCT AGC AAA GG-3′ and 5′-A TAA GAA TGC GGC CGC TTT GTA GAG CTC ATC-3′, which resulted in the introduction of 5′ and 3′ *Not*I sites. The PCR product was digested with *Not*I and subcloned into pCMV-PV-Myc-Nuc to yield an in-frame GFP fusion (pCMV-PV-GFP-Myc-Nuc). The final resulting fusion protein was designated PV-NLS-GFP.

The cytoplasmically targeted PV expression vector was constructed by subcloning the same *Sal*I/*Not*I fragment of full-length rat PV cDNA into the pCMV-Myc-Cyto vector (Invitrogen), as described for pCMV-Myc-Nuc. This construct was designated pCMV-PV-Myc-Cyto and was then used to generate a GFP fusion with PV. GFP was subcloned in-frame at the carboxyl terminus of PV using the GFP-specific primers described above. Next, the *Sal*I site was removed from the plasmid backbone by *in vitro* mutagenesis using the QuikChange mutagenesis procedure as described by the manufacturer (Stratagene, La Jolla, CA). The complete coding region of the PV-GFP-Myc fusion protein was amplified using oligonucleotide primers (5′-GGG GTC GAC GCA TTA CAA AAA AAA TTA GAA GAA TTA GAA TTA GAT GAA ATG TCG ATG ACA GAC-3′ and 5′-GCG AGC TTC TAG ACT ATG CGG CCC C-3′) to introduce the nuclear exclusion signal (NES) sequence derived from the MKK1 (46, 47). The NES sequence derived from MKK1 with this PV fusion encoded a short stretch of amino acids that represent residues 32–44 of MEK1, which does not contain the putative ERK binding site. These primers also introduced *Sal*I and *Xba*I sites, which were used to subclone this DNA fragment into pCMV-Myc-Cyto to generate PV-NES-GFP.

Site-directed mutagenesis was carried out to generate the mutant parvalbumins PV-NLS-CD-GFP and PV-NLS-CDEF-GFP coding for proteins in which either one or both of the functional Ca^{2+}-binding sites (CD or EF domain) were inactivated by substituting a glutamate for a valine residue at position 12 of each Ca^{2+}-binding loop (48). The PV-

NLS-GFP DNA was used as a template for mutagenesis. The following synthetic oligonucleotides containing mismatches in codon 62 of the CD loop or in codon 101 of the EF loop were used: CD_{62}, 5′-GC TTC ATT GAG GAG GAT GTG CTG GGG TCC ATT CTG-3′, and EF_{101}, 5′-GGC AAG ATT GGG GTT GAA GTG TTC TCC ACT CTG GTG GCC-3′ (mutated residues are underlined). The sequences of PV-NLS-CD-GFP and PV-NLS-CDEF-GFP were confirmed by automated DNA sequencing.

Cytosolic and Nuclear Ca^{2+} Measurements—Two types of Ca^{2+} measurements were made. Base-line measurements of Ca_{cyt}^{2+} and Ca_{nuc}^{2+} were performed with the ratiometric Ca^{2+} indicators indo-1 and fura-2. Measurements of agonist-induced changes in Ca_{cyt}^{2+} and Ca_{nuc}^{2+} over time were performed with rhod-2, fura-2, or fluo-4. In preparation for all experiments, cells were plated onto glass coverslips and transfected 48 h in advance with PV-NLS-GFP, PV-NES-GFP, or PV-NLS-CD-GFP. The cells were loaded with 5–6 μM of the acetoxymethyl (AM) forms of the respective indicators (Molecular Probes, Eugene, OR) for 30–60 min at 37 °C. Indo-1-loaded cells were studied by two-photon microscopy, and rhod-2- or fluo-4-loaded cells were studied using confocal microscopy. A Bio-Rad MRC-1024 combined confocal and two-photon microscope was used for both of these experiments. Fura-2 fluorescence was observed by epifluorescence microscopy using a charge-coupled device camera connected to a PC-based imaging system for analysis of ratio measurements (Spectralyzer, Thomas Jefferson University, Fluorescence Imaging Laboratory, Philadelphia, PA or Axon Imaging Workbench, Axon Instruments, Foster City, CA).

For two-photon imaging, a femtosecond-pulsed Tsunami Ti:Sapphire laser (Spectra-Physics, Mountain View, CA) was used as described previously (49). Here, two-photon microscopy was used to excite the dual wavelength Ca^{2+}-sensitive fluorescent indicator indo-1 (50, 51). Indo-1-loaded cells were transferred to a chamber on the stage of a Zeiss Axiovert microscope, which used a 63 × 1.4 N.A. oil immersion objective, and the cells were perfused with a Hepes-buffered solution. The Ti:Sapphire laser was tuned to a wavelength of 720 nm, which is optimal for two-photon excitation of indo-1 (51). Emission signals were detected at two wavelengths (360–430 and 445–505 nm) using custom-made external photomultiplier tube detectors (Multiphoton Peripherals, Ithaca, NY). The images were generated from the ratio of the lower wavelength image divided by the higher wavelength image.

Time lapse confocal imaging was performed as described previously (52). Ca^{2+} transients were evoked by perfusing with buffer containing 10 μM ATP or 0.25 μM ionomycin. Cells loaded with the single wavelength Ca^{2+} dye rhod-2 (53) were first excited with the 488-snm line of a 15 mW krypton/argon laser to detect GFP fluorescent cells and subsequently with the 568-nm line to monitor rhod-2 fluorescence in these and nearby control cells. The emitted light was collected at 522/30 nm and 605/30 nm, respectively. The regions of interest were simultaneously monitored within the nucleus and cytoplasm of transfected and untransfected control cells in the same field and followed over time using Bio-Rad Timecourse software. The fluorescence intensity was displayed as arbitrary units, from which background fluorescence intensity was subtracted. The amplitude of an evoked response was defined as the difference between the peak and base-line fluorescence. Most of the variability affecting fluorescent image intensity (uneven dye loading, leakage of dye, photobleaching, and differences in machine settings) was eliminated by comparing transfected cells only to untransfected controls in the same field.

For the experiments involving fura-2, the fluorescent images were obtained alternately at 340- and 380-nm excitation wavelengths with an emission wavelength of 460 to 640 nm. After correction for background fluorescence, Ca^{2+} transients in both nucleus and cytosol of individual cells were expressed as the 340/380 nm fluorescence ratio.

Immunofluorescence—For parvalbumin immunofluorescence, the cells were methanol-fixed and co-labeled with propidium iodide. For triple labeling experiments, 293 cells were serum-starved for 24–48 h and then left unstimulated or treated with 100 ng/ml EGF for 15 min prior to fixation in 4% paraformaldehyde. After blocking in phosphate-buffered saline containing 3% bovine serum albumin, the cells were incubated with primary antibodies for at least 2 h or overnight. The primary antibodies used were polyclonal anti-phospho-Elk-1 (1:100; Cell Signaling, Beverly, MA) and polyclonal anti-phospho-pERK1/2 (1:100; Cell Signaling). Monoclonal antibodies to the HA (1:1000) and FLAG (10 μg/ml) epitopes were obtained from Covance (Princeton, NJ) and Sigma, respectively. Primary antibodies were detected by incubation with Cy3-conjugated anti-rabbit IgG and Cy5-conjugated anti-mouse IgG from Jackson ImmunoResearch (West Grove, PA).

Analysis of ERK Activation and Elk-1 Phosphorylation—To determine the phosphorylation status of ERK, 293 cells were transiently

transfected with 1 μg of pCG-HA-ERK2, and either 9 μg of pCMV-Myc-Cyto-GFP (GFP), 6 μg of PV-NLS-GFP, 9 μg of PV-NES-GFP, 9 μg of PV-NLS-CD-GFP, or 6 μg of pMT2-H-Ras (V12) as indicated. 293 cells were either left unstimulated or stimulated with 10 ng/ml EGF for the indicated times. The cells were washed twice with ice-cold phosphate-buffered saline and lysed in 1 ml of Nonidet P-40 lysis buffer (1.0% Nonidet P-40, 50 mM Tris-HCl, pH 7.4, 150 mM NaCl, 5 mM EDTA, 5 μg/ml leupeptin, 5 μg/ml aprotinin, 1 μg/ml pepstatin A, 1 mM phenyl-methylsulfonyl fluoride, 1 mM benzamidine, 2 mM NaVO₃, and 50 mM NaF). The cell lysates were cleared by centrifugation at 4 °C at 14,000 rpm for 10 min. The protein concentration was determined using Coomassie protein reagent (Pierce). Approximately 0.5–1 mg of cell lysates were incubated overnight with 5 μg of anti-HA monoclonal antibody (Roche Molecular Biochemicals), and the immune complexes were collected on protein A-Sepharose for 1 h. The immune complexes were washed twice with 500 μl of ice-cold Nonidet P-40 lysis buffer (containing 2 mM NaVO₃ and 5 mM NaF), followed by two washes with 500 μl of ice-cold ST buffer (150 mM NaCl and 50 mM Tris-HCl, pH 8, containing 2 mM NaVO₃ and 5 mM NaF). The immune complexes were resolved by SDS-PAGE, and the proteins were transferred to Immobilon-P membranes (Millipore, Bedford, MA) and immunoblotted with anti-phospho-ERK and anti-ERK1/2 antibodies (Santa Cruz Biotechnology, Santa Cruz, CA).

The effects of Elk-1 phosphorylation were determined by transiently transfecting 293 cells with 1 μg of Elk-1-FLAG (kindly provided by Dr. Andrew Sharrocks, University of Manchester, Manchester, UK), and 5 μg of GFP, 3 μg of PV-NLS-GFP, 5 μg of PV-NES-GFP, 5 μg of PV-NLS-CD-GFP, or 3 μg of H-Ras (V12) as indicated. GFP was used as filler DNA to normalize the total amount of transfected DNA. The cells were then either left unstimulated or stimulated with 10 ng/ml EGF or 0.25 μM ionomycin for the indicated times, washed twice with ice-cold phosphate-buffered saline, and lysed in 500 μl of 1× sample buffer. The cell lysates were resolved by SDS-PAGE, transferred to Immobilon-P membranes, and subjected to immunoblotting with anti-phospho(Ser³⁸³)-Elk-1 (Cell Signaling) and anti-FLAG (Sigma) antibodies. Immunoblots were controlled for protein loading by Ponceau S staining of transferred proteins on the Immobilon membrane. Primary antibodies were detected using peroxidase-conjugated secondary antibodies and enhanced chemiluminescence (Amersham Biosciences).

Elk-1 Transactivation Assay—Elk-1 luciferase activity was measured using a luciferase assay system kit from Promega (Madison, WI) according to the manufacturer's instructions. 293 or HepG2 cells were co-transfected with 0.5 μg of Elkc-GAL4 (Elkc), 0.5 μg of 5X-GAL4-Luc, 0.5 μg of SV-40 β-galactosidase, and either 5 μg of GFP, 3 μg of PV-NLS-GFP, 5 μg of PV-NES-GFP, or 5 μg of PV-NLS-CD-GFP as indicated. Serum-starved 293 cells were left unstimulated or stimulated with either 10 ng/ml EGF or 0.25 μM ionomycin for 5 h. HepG2 cells were stimulated with either 100 ng/ml EGF or 0.5 μM ionomycin for 4 h. To determine the requirement of intracellular Ca²⁺ for EGF-induced Elk-1 transactivation, HepG2 cells were transfected with 0.5 μg of Elkc, 0.5 μg of 5X-GAL4-Luc, 0.5 μg of SV-40 β-galactosidase, and 3 μg of GFP. The cells were pretreated with either vehicle control (Me₂SO) or BAPTA-AM (30 μM) (Molecular Probes) for 20 min prior to stimulation with 100 ng/ml EGF for 4 h. Luciferase and β-galactosidase activities were determined, and the luciferase values were normalized to β-galactosidase.

Statistical Analysis—The data are given as the mean values ± S.E. Groups of data were compared using one-way repeated measures analysis of variance or one-way analysis of variance. When significant overall effects were found, post-test comparisons between selected groups were made using the Bonferroni multiple comparison tests. A p value of <0.05 was considered to indicate statistically significant differences. Statistical analyses were performed with the PRISM statistical software program (GraphPad, San Diego, CA).

RESULTS

Expression and Subcellular Localization of Targeted Parvalbumin-GFP Fusion Proteins—Previous experiments designed to selectively block Ca²⁺ signaling in the nucleus have utilized microinjection techniques to deliver a nondiffusible Ca²⁺ chelator into this subcellular compartment (21, 22). We took an alternative approach to block Ca²⁺ in distinct subcellular compartments by using the Ca²⁺-binding protein PV fused to targeting sequences that direct its subcellular localization to either the nucleus or cytosol. Although PV has been demonstrated to inhibit Ca²⁺ signaling when expressed in mamma-

lian cells (54, 55), targeted expression of PV to discrete subcellular compartments to locally buffer Ca²⁺ has not been reported. Nuclear expression of PV was established by generating an in-frame fusion of PV with the nuclear localization signal derived from the SV40 large T antigen (56) (Fig. 1*A*). Cytosolic expression of PV was established by generating a fusion protein of PV with the NES derived from the MKK1 (46, 47) (Fig. 1*A*). Subcellular localization and expression of the nuclear and cytosolically targeted PV proteins were detected by fusion with GFP. Immunoblotting for PV in PV-NLS-GFP and PV-NES-GFP COS-1 transfectants confirmed expression of the appropriate molecular weight PV fusion proteins, whereas controls showed no immunoreactivity (Fig. 1*B*). Confocal imaging of PV-NLS-GFP- and PV-NES-GFP-transfected HepG2 cells verified nuclear and cytoplasmic localization of PV-NLS-GFP and PV-NES-GFP proteins, respectively (Fig. 1*C*).

Targeted PV as a Selective Buffer of Ca²⁺$_{cyt}$ and Ca²⁺$_{nuc}$—To determine whether targeted PV selectively buffers Ca²⁺ in either the nucleus or cytosol, we examined the effects of PV expression on ATP-induced Ca²⁺ increases in both the nucleus and cytosol of HepG2 cells. ATP elicits a robust increase in intracellular free Ca²⁺ via activation of purinergic P2Y receptors and subsequent inositol 1,4,5-trisphosphate formation (57, 58). Ca²⁺$_{nuc}$ and Ca²⁺$_{cyt}$ were detected with the long wavelength indicator dye rhod-2 to avoid interference from GFP fluorescence. HepG2 cells expressing PV-NLS-GFP were stimulated with ATP (10 μM), which increased rhod-2 fluorescence to similar levels in the cytosol of both PV-NLS-GFP-transfected and untransfected HepG2 cells (Fig. 2, *A*, *left panel*, and *C*). However, ATP-induced increases in nuclear fluorescence were reduced in PV-NLS-GFP-transfected HepG2 cells, as compared with the increases in nuclear fluorescence observed in untransfected control cells (Fig. 2, *A*, *right panel*, and *C*; $n = 44$, $p < 0.01$). In contrast, expression of PV-NES-GFP suppressed ATP-induced increases in rhod-2 fluorescence in the cytosol relative to untransfected controls ($n = 31$, $p < 0.001$) but did not affect the rise in the nucleus (Fig. 2, *B* and *C*). Expression of GFP alone had no effect on ATP-induced Ca²⁺ signals (data not shown). These results demonstrate that expression of PV in either the nucleus or cytoplasm selectively suppresses agonist-induced Ca²⁺ transients in the targeted cellular compartment.

In addition to agonist-induced Ca²⁺ signals, base-line measurements using the ratiometric Ca²⁺ indicators indo-1 or fura-2 were performed. To avoid potential interference of the GFP fluorescence with fura-2 and indo-1 fluorescence, we used PV-NLS instead of PV-NLS-GFP. The cells were co-transfected with red fluorescent protein, because this fluorophore is compatible with the use of these fluorescent dyes and thus let us distinguish the transfected cells from untransfected control cells. Basal levels of Ca²⁺ in the nucleus were not significantly lower in cells expressing PV-NLS cells, relative to PV-negative control cells (Fig. 3; $n = 10$, $p = 0.39$). These results were confirmed using indo-1 and two-photon imaging (data not shown).

EGF-mediated Elk-1 Transactivation Requires Intracellular Ca²⁺—Engagement of the EGF signaling pathway results in the activation of ERK and subsequent transactivation of the ETS domain-containing transcription factor Elk-1 (23). To determine the requirement for Ca²⁺ in EGF-mediated activation of Elk-1, total free cellular Ca²⁺ was buffered using the intracellular Ca²⁺ chelator BAPTA-AM. To assess the ability of EGF to induce Elk-1 transactivation, we utilized a chimera representing the carboxyl terminus of Elk-1 (amino acids 307–428) fused to the DNA-binding domain of the GAL4 transcription factor. Previously, it has been shown that this Elk-1-GAL4 chimera undergoes MAPK-induced phosphorylation and leads

FIG. 1. **Expression and subcellular localization of targeted PV-GFP fusion proteins.** *A*, schematic representation of the targeted PV-GFP expression vectors. Rat PV cDNA was fused to a targeting signal (NLS or NES), GFP, and the c-Myc epitope (*Myc*). *B*, immunoblotting of PV-GFP constructs. COS cells were transfected with expression vectors for PV-NLS-GFP, PV-NES-GFP, or vector control (GFP). Total cellular proteins were separated on SDS-PAGE and immunoblotted with a monoclonal anti-PV antibody. PV-NLS-GFP and PV-NES-GFP direct expression of the ~40-kDa fusion proteins. *C*, subcellular localization of the indicated PV-GFP constructs using confocal microscopy. *Green* indicates GFP, *red* indicates the nuclear stain propidium iodide, and *yellow* indicates co-localization of the two signals. Expression of PV-NLS-GFP is restricted to the nucleus, whereas PV-NES-GFP is uniformly distributed throughout the cytosol but excluded from the nucleus.
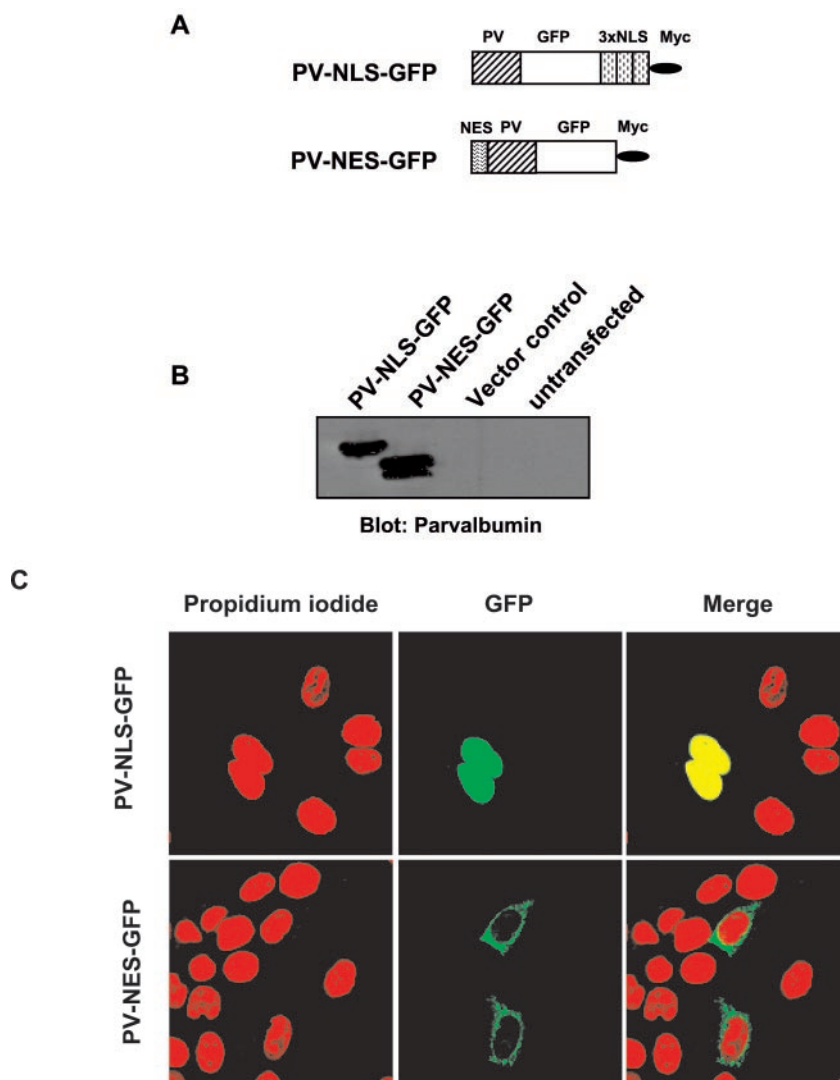
to the transcriptional activation of a luciferase reporter driven by five GAL4 DNA-binding element repeats (5X-GAL4-Luc) (32). HepG2 cells were co-transfected with Elkc-1-GAL4 (Elkc), 5X-GAL4-Luc, and β-galactosidase as a control. These transfected cells were serum-starved for 48 h. Prior to EGF stimulation, transfected HepG2 cells were pretreated for 20 min with either Me$_2$SO (control condition) or BAPTA-AM (30 μM) to chelate intracellular Ca^{2+}. HepG2 cells were subsequently stimulated with EGF (100 ng/ml) for 4 h, and the activity of Elk-1-mediated luciferase activity was determined. These data showed that EGF-mediated Elk-1 transactivation was induced 1.6-fold relative to unstimulated HepG2 cells (Fig. 4). However, in HepG2 cells pretreated with BAPTA-AM, the ability of EGF to induce Elk-1 transactivation was completely inhibited (Fig. 4; $p < 0.001$). These results demonstrate that intracellular Ca^{2+} is required for EGF-induced Elk-1 transactivation in HepG2 cells.

EGF-mediated Elk-1 Transactivation Requires Nuclear but Not Cytosolic Ca²⁺—EGF is known to mobilize Ca^{2+} from intracellular Ca^{2+} stores by activation of phospholipase Cγ and subsequent inositol 1,4,5-trisphosphate formation in primary hepatocytes (59) and also in several cell lines including A431 human epidermoid carcinoma (36) and renal epithelial cells (60). To determine whether EGF induces Ca^{2+} signals in both the cytosol and nucleus of HepG2 cells, serum-deprived cells loaded with fura-2 were stimulated with 50–60 ng/ml EGF, and changes in Ca$^{2+}_{cyt}$ and Ca$^{2+}_{nuc}$ were monitored by epifluores-

cence microscopy ratio imaging. Fig. 5*A* shows a typical Ca^{2+} response in the two compartments during EGF stimulation. It is clear that EGF induced significant increases in both Ca$^{2+}_{nuc}$ and Ca$^{2+}_{cyt}$.

To determine the relative contribution of Ca$^{2+}_{nuc}$ and Ca$^{2+}_{cyt}$ to EGF-mediated Elk-1 transactivation, we utilized the targeted PV constructs. HepG2 cells were co-transfected with a control vector (GFP), PV localized to the nucleus (PV-NLS-GFP), or PV localized to the cytosol (PV-NES-GFP), along with Elkc, 5X-GAL4-Luc, and β-galactosidase. HepG2 cells were serum-starved for 48 h and were then restimulated with EGF (100 ng/ml) for 4 h. As observed previously (Fig. 4), EGF stimulation of HepG2 cells resulted in a 2-fold increase in Elk-1 transactivation (Fig. 5*B*). However, EGF-induced Elk-1 transactivation was completely inhibited in HepG2 cells that expressed PV-NLS-GFP (Fig. 5*B*; $p < 0.05$). In contrast, buffering the cytosolic pool of Ca^{2+} with PV-NES-GFP did not exhibit any appreciable diminution in the ability of EGF to activate Elk-1 ($p > 0.05$). These data demonstrate that targeted expression of PV to the nucleus, but not the cytosol, inhibits EGF-induced Elk-1 transactivation (Fig. 5*B*). Taken together with the experiments in Fig. 4, these data strongly suggest that nuclear Ca^{2+} is required for the appropriate transactivation of Elk-1 in response to EGF in HepG2 cells.

Generation of a Nuclear Localized Ca²⁺-binding Deficient Mutant of Parvalbumin—To determine whether the inhibitory effects of expressing PV in the nucleus specifically are due to its
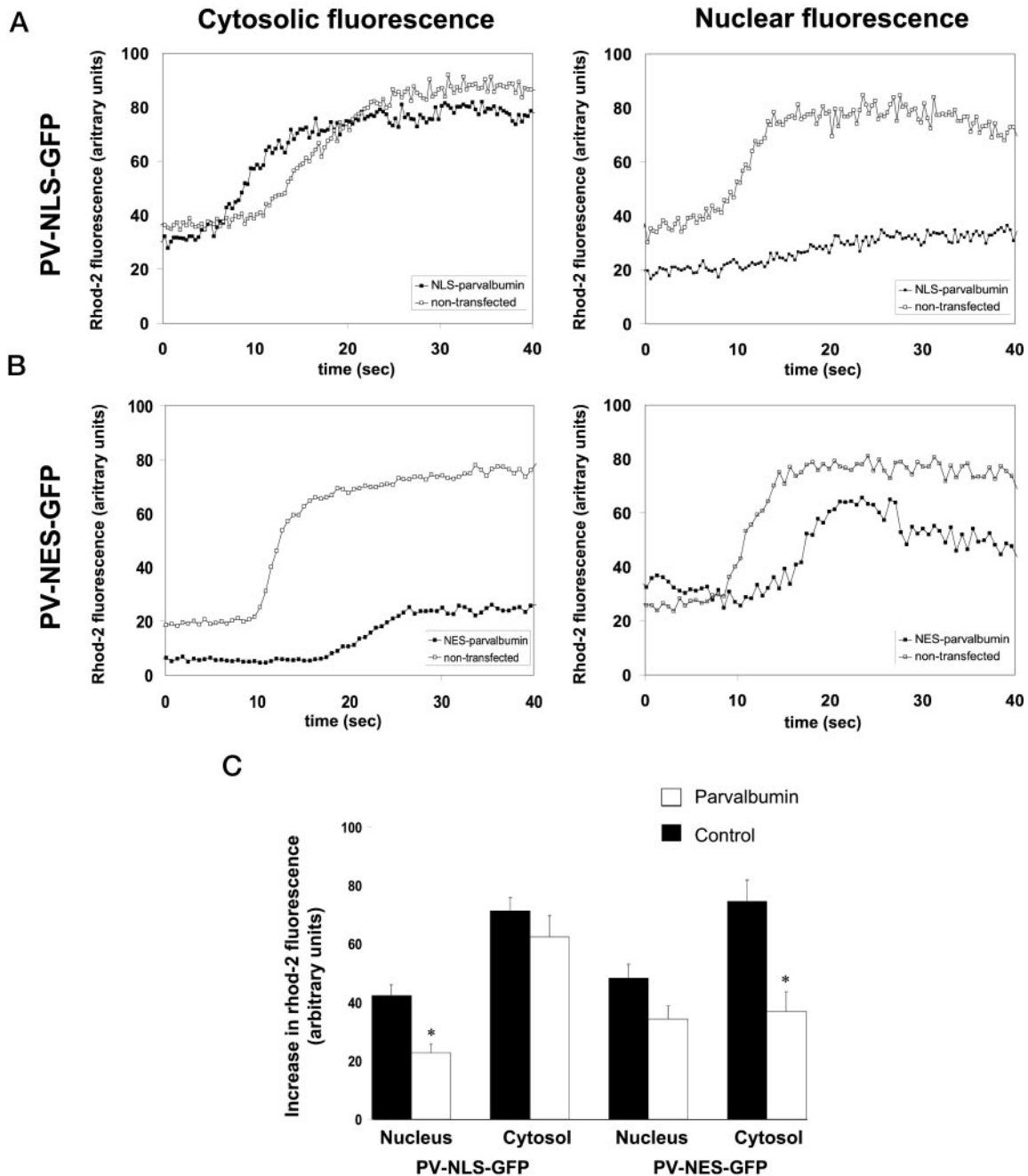
FIG. 2. **ATP-induced increases in Ca$^{2+}_{nuc}$ or Ca$^{2+}_{cyt}$ are selectively blocked in HepG2 cells expressing either PV-NLS-GFP or PV-NES-GFP.** *A*, PV-NLS-GFP attenuates ATP-induced increases in Ca$^{2+}_{nuc}$ but not Ca$^{2+}_{cyt}$. HepG2 cells expressing PV-NLS-GFP along with untransfected controls were loaded with rhod-2 and stimulated with ATP (10 μM). Similar increases in rhod-2 fluorescence were observed in the cytosol of the transfected and untransfected cell (*left panel*). A large, rapid increase in nuclear rhod-2 fluorescence was observed in the untransfected cell, whereas the increase in nuclear fluorescence was markedly attenuated in a nearby cell expressing PV-NLS-GFP (*right panel*). *B*, PV-NES-GFP attenuates ATP-induced increases in Ca$^{2+}_{cyt}$ but not Ca$^{2+}_{nuc}$. HepG2 cells expressing PV-NES-GFP along with untransfected controls were loaded with rhod-2 and stimulated with ATP (10 μM). ATP-induced increases in cytosolic rhod-2 fluorescence were markedly reduced in the PV-NES-GFP-transfected cell (*left panel*). Similar increases in rhod-2 fluorescence were observed in the nucleus of the transfected and a nearby untransfected control cell (*right panel*). *C*, summary of rhod-2 measurements. The data represent the means $\pm$ S.E. of the increase in fluorescence ($\Delta F = F_{max} - F_{baseline}$) observed in 44 cells expressing PV-NLS-GFP and 31 cells expressing PV-NES-GFP, plus 1–7 control cells in the same field. The *asterisks* indicate significant differences compared with untransfected controls.

Ca^{2+} buffering capacity, a nuclear localized mutant form of PV that has reduced Ca^{2+} buffering capacity was generated. Site-directed mutagenesis was used to inactivate either one or both of the Ca^{2+}-binding sites in the paired EF hand sites of this protein (61). PV-NLS-CD-GFP contained an E62V substitution in the CD Ca^{2+}-binding site but maintained an active EF Ca^{2+}-binding site. The double mutant PV-NLS-CDEF-GFP, containing E62V/E101V substitutions, was engineered to inactivate both CD and EF sites. Because these mutations might

affect the ability of the parvalbumin antibody to recognize its epitope, the monoclonal 9E10 c-Myc antibody was used to detect the tagged fusion proteins. Immunoblotting of wild-type and mutated PV constructs in SK-HEP-1 cell transfectants showed that expression of PV-NLS-CD-GFP was reduced compared with wild-type PV-NLS-GFP, whereas the doubly defective mutant PV-NLS-CDEF-GFP showed little or no detectable expression (Fig. 6A). Ideally, the mutant of PV that was completely crippled in its Ca^{2+}-binding capacity would have been
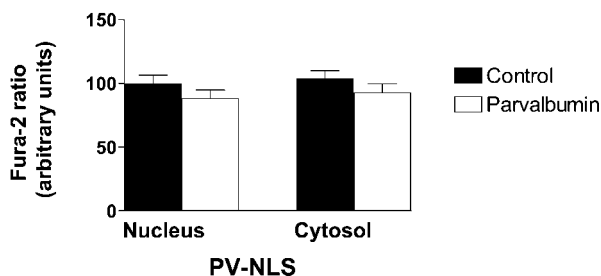
FIG. 3. **Basal Ca$^{2+}_{nuc}$ is unaffected in cells expressing PV-NLS.** Control SK-HEP-1 cells and cells co-transfected with PV-NLS and red fluorescent protein were loaded with fura-2 and analyzed by fluorescence ratio imaging. The data represent the means ± S.E. obtained from 10 cells expressing PV-NLS and 25 PV-negative control cells.
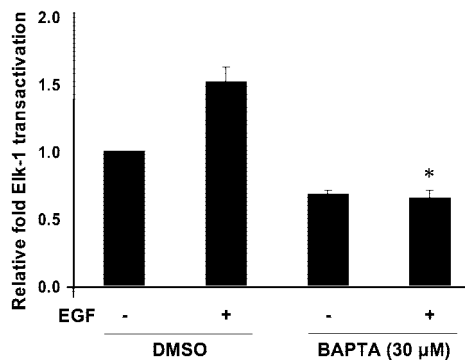

FIG. 4. **EGF-induced Elk-1 transactivation in HepG2 cells is dependent upon intracellular Ca^{2+}.** HepG2 cells were rendered quiescent by serum deprivation and were pretreated with either 30 μM BAPTA-AM or dimethyl sulfoxide (*DMSO*) vehicle control for 20 min prior to EGF (100 ng/ml) stimulation for 4 h. The lysates were prepared from these cells, and the activities of luciferase and β-galactosidase were determined. The data shown represent the fold change in Elk-1 transactivation relative to that of the unstimulated vector control, derived from the normalized luciferase to β-galactosidase activities. The results represent the means ± S.E. from five separate experiments performed in triplicate. The *asterisk* indicates a significant difference ($p < 0.001$) compared with EGF-stimulated DMSO control.

FIG. 5. **Expression of PV-NLS-GFP inhibits EGF-induced Elk-1 transactivation in HepG2 cells.** *A*, EGF increases Ca^{2+} in both the nucleus and cytosol of HepG2 cells. HepG2 cells loaded with fura-2 were stimulated with 50–60 ng/ml EGF, and the EGF-induced Ca^{2+} responses in the nuclear and cytosolic compartment were monitored by epifluorescence microscopy ratio imaging. The data shown are representative results from >10 cells. *B*, HepG2 cells were transfected with either GFP (vector control), PV-NLS-GFP, or PV-NES-GFP and were serum-deprived for 48 h prior to stimulation with EGF (100 ng/ml) for 4 h. The data shown represent the fold change in Elk-1 transactivation relative to that of the unstimulated vector control, derived from the normalized luciferase to β-galactosidase activities. The results represent the means ± S.E. from five separate experiments performed in triplicate. The *asterisk* indicates a significant difference ($p < 0.05$) compared with EGF-stimulated GFP control.

the most appropriate control. However, as a result of the poor expression of this mutant, the single Ca^{2+}-binding site defective PV mutant was used for subsequent studies. Confocal immunofluorescence confirmed the nuclear localization of PV-NLS-CD-GFP (Fig. 6*B*).

To examine the effect of PV-NLS-CD-GFP on Ca^{2+} transients, transfected HepG2 cells were stimulated with ATP (10 μM) and monitored as described for wild-type PV. No significant differences were found in the ATP-induced rises in cytosolic fluorescence of PV-NLS-CD-GFP-transfected cells and untransfected control cells (data not shown; $n = 50$, $p > 0.05$). However, ATP-induced increases in nuclear fluorescence were reduced in PV-NLS-CD-GFP-transfected HepG2 cells, as compared with untransfected control cells (Fig. 7; $n = 50$, $p < 0.01$), although to a lesser extent than in PV-NLS-GFP-transfected cells (Fig. 7; $n = 44$, $p < 0.001$). These results thus indicate that the mutant PV-NLS-CD-GFP exhibits a reduced ability to buffer Ca^{2+} as compared with that of wild-type parvalbumin. Therefore, this mutant PV protein was used to determine whether the observed effects of PV expression are solely due to its Ca^{2+} binding properties.

A Ca^{2+}-binding Deficient Mutant of Parvalbumin Targeted to the Nucleus Fails to Block EGF-mediated Elk-1 Transactivation—To demonstrate that the inhibitory effects of PV-NLS-GFP on EGF-mediated Elk-1 transactivation were due specifically to the ability of PV to buffer Ca^{2+}, we used the Ca^{2+}-binding deficient mutant of PV. Because EGF induced Elk-1 transactivation by only 2-fold in HepG2 cells (Figs. 4 and 5), we
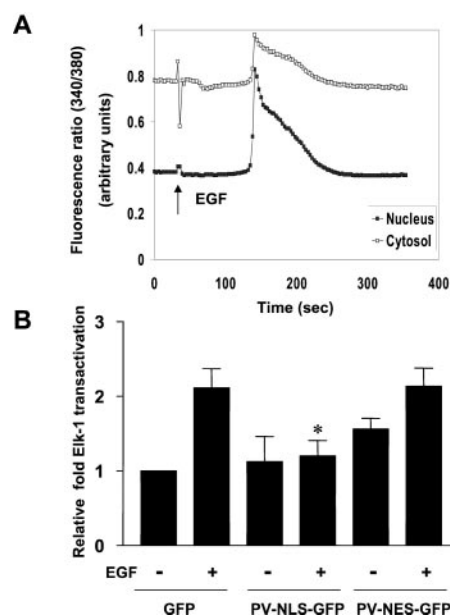
also examined the magnitude of EGF-induced Elk-1 transactivation in human embryonic kidney 293 cells. We first examined nuclear and cytosolic Ca^{2+} signaling in 293 cells following EGF stimulation. Fura-2 ratio imaging of 293 cells revealed that both nuclear and cytosolic Ca^{2+} levels are increased by EGF (Fig. 8*A*). Second, EGF-induced Elk-1 transactivation was substantially more robust than that of HepG2 cells, resulting in a 6–7-fold level of Elk-1 transactivation as compared with controls (Fig. 8*C*). Thus, 293 cells appeared appropriate for our analysis of the effects of PV-NLS-GFP and PV-NLS-CD-GFP on EGF regulation of Elk-1.

Because the steady-state expression level of PV-NLS-CD-GFP was lower than that of PV-NLS-GFP (Fig. 6*A*), we performed a titration with increasing amounts of these expression vectors. This permitted us to use appropriate levels of cDNA for transfections to achieve comparable levels of protein expression. As shown in Fig. 8*B*, a comparable level of expression of PV-NLS-GFP to PV-NLS-CD-GFP was achieved at a ratio of ~1 to 2 for PV-NLS-GFP to PV-NLS-CD-GFP, respectively. 293 cells were transiently transfected using these ratios of PV-NLS-GFP and PV-NLS-CD-GFP along with PV-NES-GFP, Elkc, 5XGAL4-Luc, and a β-galactosidase control. Although EGF stimulation of 293 cells expressing GFP resulted in a 6-fold activation of Elk-1, expression of PV-NLS-GFP reduced this to a 3-fold Elk-1 transactivation (Fig. 8*C*). This represents an inhibition by ~50% relative to the GFP-transfected controls ($p < 0.05$). In contrast, expression of PV-NLS-CD-GFP failed to inhibit EGF-stimulated Elk-1 transactivation relative to that of GFP vector control ($p > 0.05$). These data demonstrate that inhibition of Elk-1 transactivation by PV in the nucleus is solely due to the ability of PV to buffer Ca^{2+}. Finally, as with

A

Blot: c-myc

B

FIG. 6. **Expression and subcellular localization of Ca²⁺ binding-deficient PV mutants.** *A*, immunoblotting of mutant PV constructs. SK-HEP-1 cells were transfected with expression vectors for PV-NLS-GFP or PV mutants with either one (PV-NLS-CD-GFP) or two (PV-NLS-CDEF-GFP) mutated Ca²⁺-binding sites. Total cellular proteins were separated on SDS-PAGE and immunoblotted with a monoclonal anti-Myc antibody to detect expression of the tagged ~40-kDa fusion proteins. Note that expression of PV-NLS-CD-GFP is reduced compared with PV-NLS-GFP, whereas the doubly defective mutant PV-NLS-CDEF-GFP was barely expressed. *B*, nuclear localization of PV-NLS-CD-GFP. *Green* indicates GFP construct, *red* indicates the propidium iodide nuclear stain, and *yellow* indicates co-localization of the two signals.
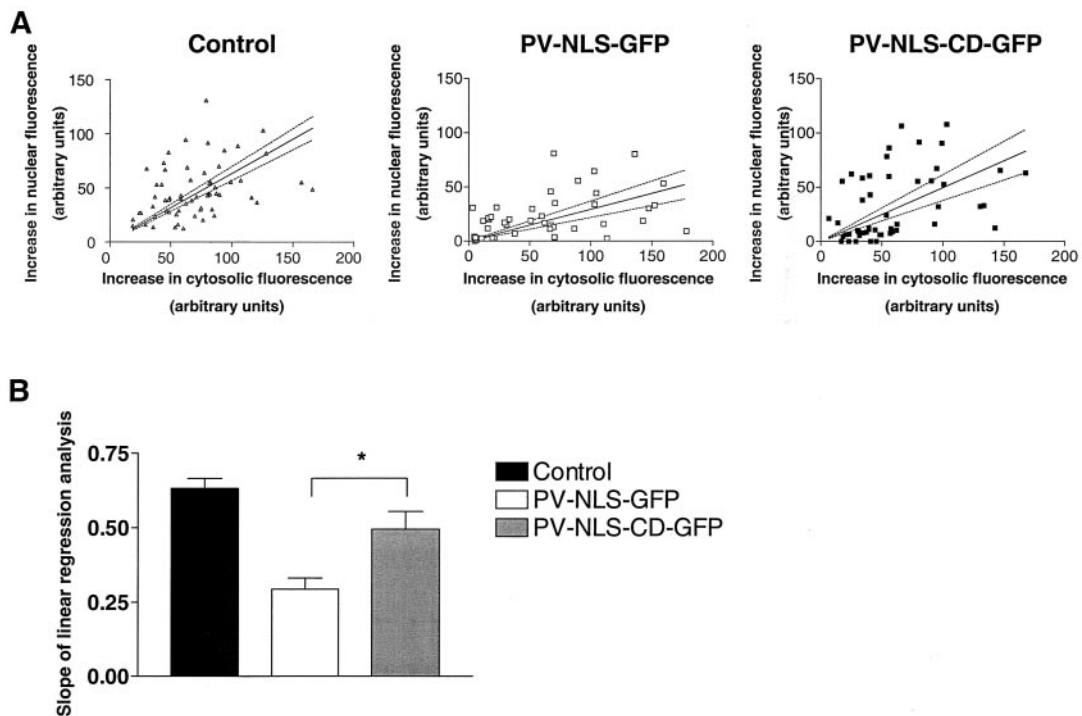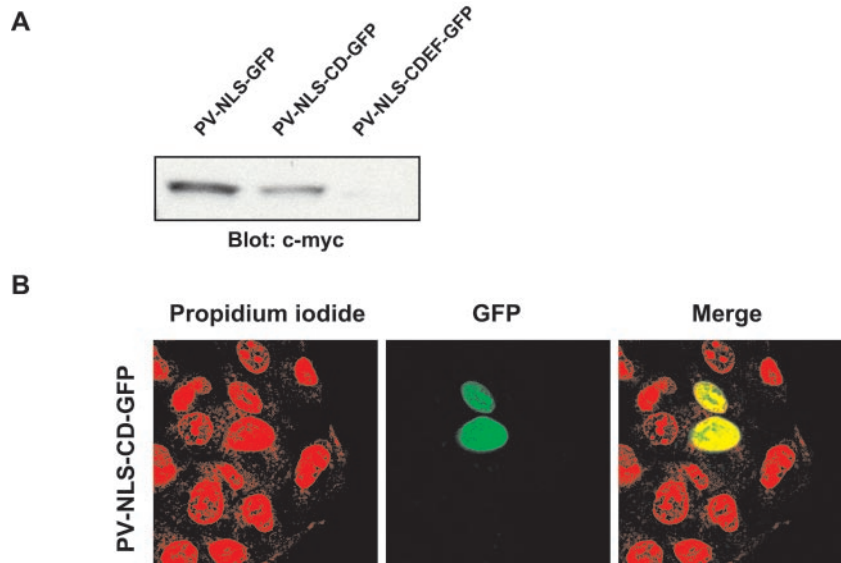
A

B

FIG. 7. **PV-NLS-CD-GFP exhibits weakened Ca²⁺ₙᵤ𝒸 buffering capacity.** HepG2 cells expressing wild-type PV-NLS-GFP or the mutant PV-NLS-CD-GFP construct along with untransfected controls were loaded with rhod-2 and stimulated with ATP (10 μM). The changes of rhod-2 fluorescence in the cytosolic and nuclear compartment were monitored using time lapse confocal microscopy. *A*, scatter plots of increase in nuclear *versus* cytosolic rhod-2 fluorescence. Each data point represents the increases in rhod-2 fluorescence in the cytosolic and nuclear compartment from an individual cell. The *solid line* is the linear regression curve for these data, whereas the *two dashed lines* surrounding the regression line define the 95% confidence interval. *B*, graphical representation of the slopes from the regression analyses. The slopes for the individual regression curves are 0.63 ± 0.03 (*n* = 94), 0.29 ± 0.04 (*n* = 44), and 0.50 ± 0.06 (*n* = 50) for control, PV-NLS-GFP, and PV-NLS-CD-GFP, respectively. The slope for the PV mutant is decreased by 30% from pair-matched controls, whereas the slope for wild-type PV is decreased by half. *, *p* < 0.05.

HepG2 cells, expression of PV-NES-GFP in 293 cells also failed to inhibit EGF-induced Elk-1 transactivation (Fig. 8*C*; *p* > 0.05). Taken together, these data provide strong evidence that nuclear rather than cytosolic Ca²⁺ is required to achieve maximal EGF-induced Elk-1 transactivation.

EGF-induced Activation and Translocation of ERK Is Not Affected by Buffering Nuclear Ca²⁺—Having demonstrated that EGF-induced Elk-1 transactivation is dependent upon nuclear Ca²⁺, we asked whether this inhibitory effect was due to the inability of EGF to induce ERK activation and/or perturb ERK translocation to the nucleus. To determine the effects of buffering nuclear Ca²⁺ on EGF-induced ERK activation and

translocation to the nucleus, 293 cells were transiently transfected with HA-tagged ERK2 and either GFP, PV-NLS-GFP, PV-NLS-CD-GFP, or PV-NES-GFP. Following serum starvation, these transfected 293 cells were stimulated with EGF (10 ng/ml) for 30 min, 1 h, or 2 h and the levels of phospho-ERK2 were assessed. As shown in Fig. 9*A*, neither expression of PV-NLS-GFP nor expression of PV-NES-GFP affected the level of EGF-induced phospho-ERK2. Expression of PV-NLS-CD-GFP also did not affect EGF-induced ERK2 phosphorylation (Fig. 9*A*). Immunoblotting lysates prepared from these transfectants for ERK2 or PV demonstrated that equal levels of both ERK2 and PV were expressed (Fig. 9*A*, *middle* and *bottom*
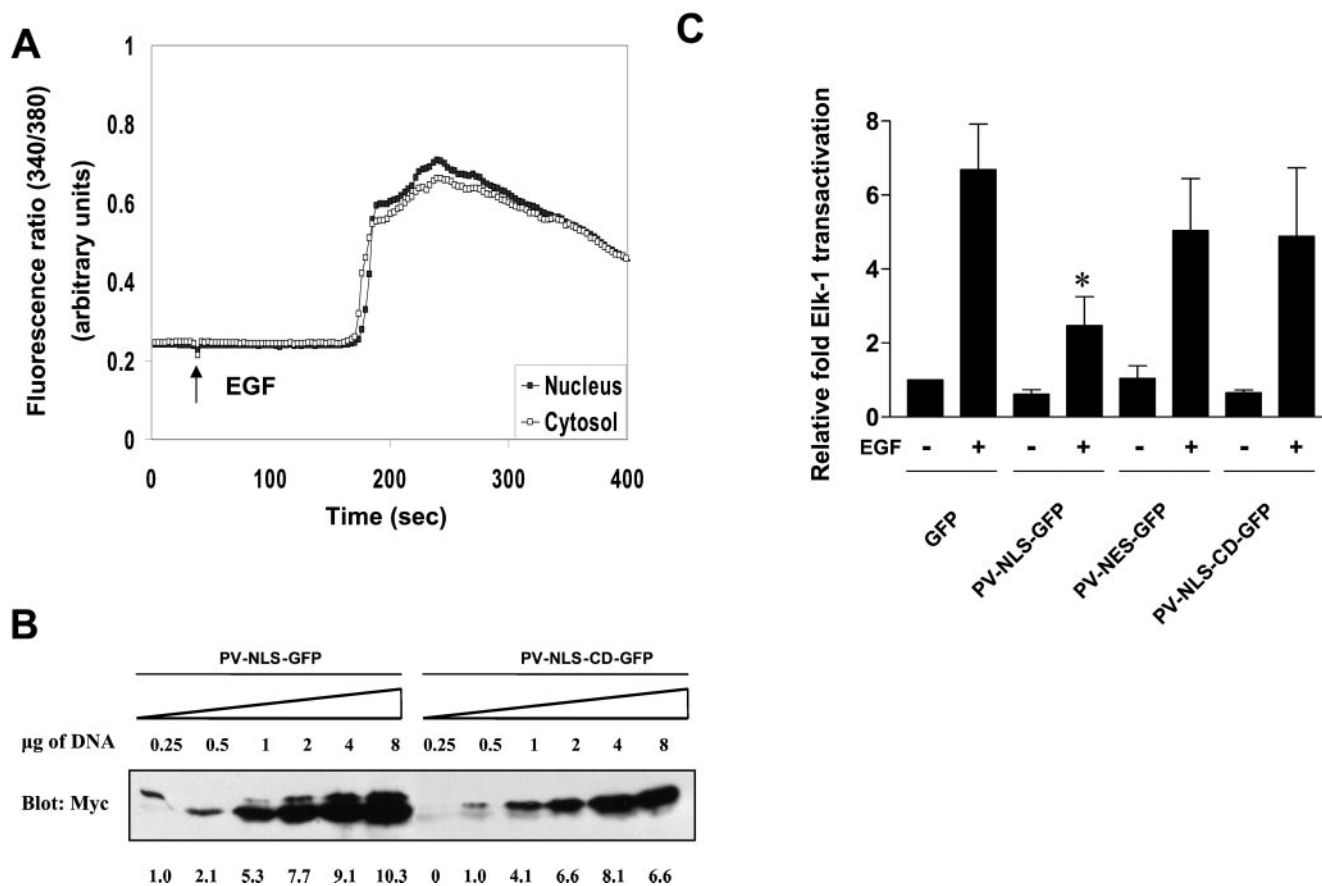
FIG. 8. **EGF-induced increase in Ca$_{nuc}^{2+}$ but not Ca$_{cyt}^{2+}$ is required for Elk-1 transactivation in 293 cells.** *A*, EGF increases Ca^{2+} both in the nucleus and cytosol of 293 cells. 293 cells loaded with fura-2 were stimulated with EGF (50–60 ng/ml), and the EGF-induced Ca^{2+} responses in the nuclear and cytosolic compartment were monitored by epifluorescence microscopy ratio imaging. The data shown are representative results from >10 cells. *B*, dose-response analysis of PV-NLS-GFP and PV-NLS-CD-GFP protein expression. 293 cells were transfected either with PV-NLS-GFP or PV-NLS-CD-GFP using the indicated amounts of cDNA. The cell lysates were prepared and immunoblotted with anti-Myc antibodies. Note that the expression of PV-NLS-CD-GFP is ~2-fold lower than PV-NLS-GFP. *C*, 293 cells were transfected with the indicated PV expression plasmids. The amount of PV-NLS-CD-GFP cDNA was ~2-fold higher than PV-NLS-GFP to obtain similar expression levels. 293 cells were rendered quiescent and then restimulated with EGF (10 ng/ml) for 5 h. The data represent the normalized luciferase to β-galactosidase units as a fold change relative to the unstimulated vector control. These data represent the means ± S.E. of five separate experiments performed in triplicate. The *asterisk* indicates a significant difference ($p < 0.05$) compared with EGF-stimulated GFP control.

panels). These results suggest that the catalytic activity of ERK is unaffected by buffering either nuclear or cytosolic Ca^{2+} independently.

To establish whether expression of PV-NLS-GFP inhibited Elk-1 transactivation by preventing translocation of ERK to the nucleus, we determined the subcellular localization of ERK2 by confocal immunofluorescence. 293 cells were co-transfected with PV-NLS-GFP and HA-ERK2 and were either left unstimulated or stimulated with EGF for 10–15 min. The localization of ERK2 and phospho-ERK was visualized using anti-ERK and anti-phospho-ERK antibodies. In unstimulated 293 cells expressing PV-NLS-GFP, ERK2 was initially excluded from the nucleus, and subsequently a fraction of ERK2 translocated to the nucleus following EGF stimulation (Fig. 9*B*). Consistent with our biochemical analysis, EGF-induced pERK was not inhibited by the expression of PV-NLS-GFP. Moreover, pERK2 was found predominantly within the nucleus of these cells. These data suggest that the inhibitory effect of PV-NLS-GFP on Elk-1 transactivation does not occur by affecting either the phosphorylation/activation or subcellular localization of ERK in response to EGF.

EGF-induced Phosphorylation and Nuclear Localization of Elk-1 Is Not Affected by Buffering Nuclear Ca^{2+}—Phosphorylation of Elk-1 on Ser[383]/Ser[389] is a key post-translational modification that regulates Elk-1 DNA binding and subsequently its transcriptional activity (31). Therefore, we hypothesized

that the inhibitory actions of PV-NLS-GFP on EGF-induced Elk-1 transactivation were due to the attenuation of Elk-1 phosphorylation. As shown in Fig. 10*A*, transient transfection of FLAG-tagged Elk-1 followed by stimulation with EGF did not inhibit its ability to become phosphorylated at Ser[383] when either PV-NLS-GFP or PV-NES-GFP was co-expressed. Again, as expected, the Ca^{2+}-deficient binding mutant did not show any effect on EGF-induced Elk-1 phosphorylation (Fig. 10*A*). Both Elk-1 and PV were expressed at equivalent levels in these transfections (Fig. 10*A*, *middle* and *bottom panels*). Finally, we determined whether expressing PV-NLS-GFP affected the nuclear localization of either Elk-1 itself or its phosphorylated form (Fig. 10*B*). 293 cells were transiently transfected with FLAG-Elk-1 and PV-NLS-GFP and either left unstimulated or stimulated with EGF. Elk-1 was localized to the nucleus in both the unphosphorylated and phosphorylated forms. This subcellular localization was not altered in cells expressing PV-NLS-GFP (Fig. 10*B*). Thus, phosphorylation of Elk-1 is not sufficient for its activation. Moreover, EGF-induced activation of Elk-1 depends not only on Elk-1 phosphorylation but also upon Ca$_{nuc}^{2+}$.

Additional Evidence That Elk-1 Phosphorylation Is Not Sufficient to Activate Elk-1 Transcription—Our data imply that Ca$_{nuc}^{2+}$ is required for EGF-mediated transactivation of Elk-1. To test whether Ca$_{nuc}^{2+}$ is also sufficient, we investigated whether ionomycin could induce Elk-1 transactivation. Treat-
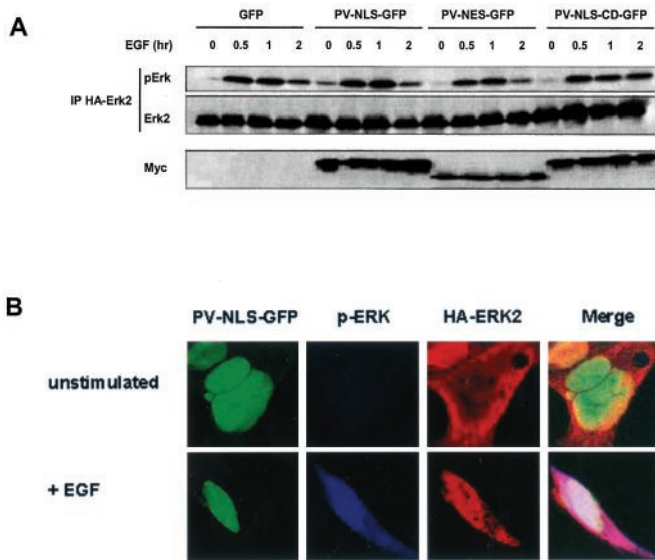
FIG. 9. **PV-NLS-GFP does not affect EGF-induced ERK phosphorylation or nuclear translocation of phospho-ERK2.** *A*, HA-tagged ERK2 was transfected into 293 cells along with either GFP, PV-NLS-GFP, PV-NES-GFP, or PV-NLS-CD-GFP. Transfected 293 cells were rendered quiescent for 24 h and then restimulated with EGF (10 ng/ml). The cell lysates were prepared at the indicated times. HA-ERK2 was immunoprecipitated (*IP*) using an anti-HA antibody, and these immune complexes were separated by SDS-PAGE and analyzed by immunoblotting with anti-phospho-ERK antibodies (*top panel*). This immunoblot was reprobed with anti-ERK antibodies (*middle panel*). PV expression levels were confirmed by immunoblotting with anti-Myc (9E10) antibodies (*bottom panel*). *B*, EGF-induced ERK translocation can occur in the presence of PV-NLS-GFP. 293 cells were co-transfected with PV-NLS-GFP and HA-ERK2. The cells were either left unstimulated or treated with EGF (100 ng/ml) for 10–15 min. Co-localization of PV-NLS-GFP (*green*), total HA-tagged ERK (*red*), and phospho-ERK (*blue*) was visualized by confocal immunofluorescence using a monoclonal anti-HA and polyclonal anti-phospho-ERK antibody, respectively. Nuclear labeling of all three fluorophores (*white*) is seen in cells stimulated with EGF.

FIG. 10. **PV-NLS-GFP does not affect EGF-induced Elk-1 phosphorylation or localization.** *A*, PV-NLS-GFP or PV-NES-GFP do not affect EGF-induced Elk phosphorylation. FLAG-tagged Elk-1 was transfected into 293 cells along with GFP vector control, PV-NLS-GFP, PV-NES-GFP, and PV-NLS-CD-GFP. Following serum deprivation for 24 h, quiescent 293 cells were stimulated with EGF (10 ng/ml), and whole cell lysates were prepared at the indicated times and separated by SDS-PAGE. The proteins were analyzed by immunoblotting with either anti-phospho (383)-Elk-1 (*top panel*) or with anti-FLAG (*middle panel*) antibodies. PV expression levels were confirmed by immunoblotting with anti-Myc (9E10) antibodies (*bottom panel*). *Lane U*, represents lysates prepared from untransfected 293 cells as a control. *B*, PV-NLS-GFP does not alter Elk-1 localization. 293 cells were co-transfected with PV-NLS-GFP and an expression vector for FLAG-Elk-1. The cells were either left unstimulated or treated with EGF for 10–15 min. Co-localization of PV-NLS-GFP (*green*), total FLAG-tagged Elk-1 (*red*), and phospho-Elk-1 (*blue*) was visualized by confocal immunofluorescence using a monoclonal anti-FLAG and polyclonal anti-phospho-Elk-1 antibodies, respectively. Nuclear labeling of all three fluorophores (*white*) is seen in cells stimulated with EGF.

ment of 293 cells with ionomycin increased both Ca$^{2+}_{cyt}$ and Ca$^{2+}_{nuc}$ (Fig. 11, *A* and *B*) and also resulted in the phosphorylation of Elk-1 (Fig. 11*C*). In contrast to EGF, ionomycin failed to stimulate transactivation of Elk-1 (Fig. 11*D*). Similar results were also observed using HepG2 cells (data not shown). Taken together, these data show that both Ca$^{2+}_{nuc}$ and Elk-1 phosphorylation are necessary but not sufficient to induce EGF-mediated transactivation of Elk-1.

DISCUSSION

Previous studies have suggested that Ca^{2+} signals in the nucleus can be regulated independently of Ca^{2+} signals in the cytosol (17, 63–66). In addition, several Ca^{2+}-dependent nuclear functions have been proposed, including apoptosis (67), nucleocytoplasmic transport of proteins (68, 69), and gene transcription (21, 22). However, the ability to study the effects of spatially distinct Ca^{2+} signaling has been technically challenging. Some investigators have employed single cell nuclear microinjection of a nondiffusible Ca^{2+} buffer to block increases in Ca$^{2+}_{nuc}$ but not Ca$^{2+}_{cyt}$ (21, 22). Although this approach has provided valuable information regarding the role of Ca$^{2+}_{nuc}$, this technique examines only single cells and thus is not conducive to performing extensive biochemical studies. The current report overcomes this limitation by using targeted expression of the Ca^{2+}-binding protein PV to selectively inhibit Ca^{2+} signaling in either the nucleus or cytosol. This strategy therefore facilitates the study of the role of subcellular Ca^{2+} signals in a variety of biological processes.

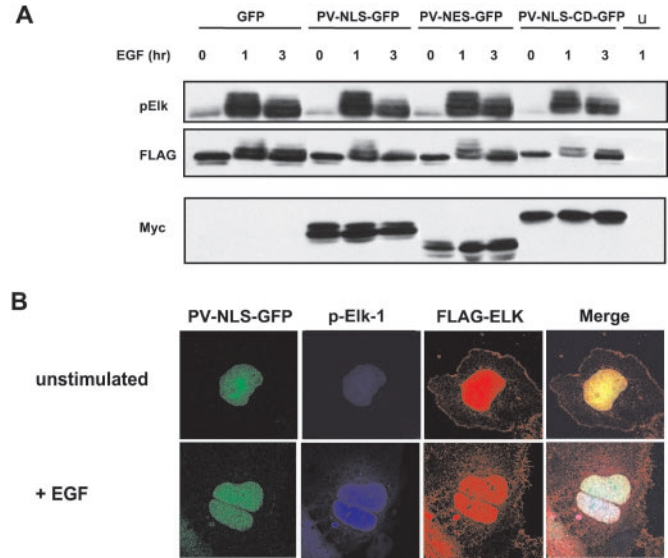PV is a high affinity Ca^{2+}-binding protein of the EF hand type with a ~10^3 higher affinity for Ca^{2+} ($K_d = 2.4 \times 10^7$ M^{-1}) than Mg^{2+} ($K_d = 2.9 \times 10^4$ M^{-1}) (70, 71). The metal-ion binding properties and crystallographic structure of PV have been described in detail (48, 61, 72). It is found at its highest concentration in quickly contracting skeletal muscle (70, 73), nervous tissue (74), kidney (75), testis (76), and endocrine glands (77). PV has been used previously as a tool to manipulate the effects of Ca^{2+} in a variety of biological processes (54, 55, 78–81). The Ca^{2+} buffering capacity of PV is thought to facilitate the relaxation of fast muscle. Expression of PV in normal and regenerating rat soleus muscle significantly shortens twitch half-relaxation time in a dose-dependent manner (78). PV gene transfer also enhances mechanical relaxation in cardiac myocytes (79). This effect is seen in the intact heart as well and has been proposed as a strategy to improve certain types of heart failure (80). A study of a PV knockout mouse has shown that the Ca^{2+} buffering action of PV also is important for the regulation of short term synaptic plasticity in gamma-amino butyric acid-responsive neurons (81). Furthermore, ectopic expression of PV in nonmuscle cell types attenuates cell cycle progression (54, 55). However, the current work is the first demonstration that targeted expression of PV can be used to examine the effects of Ca^{2+} in distinct subcellular regions.

EGF-mediated increases in Ca$^{2+}_{cyt}$ have been suggested to mediate processes such as mitogenesis, proliferation, and gene expression (82–87). However, the role specifically for Ca$^{2+}_{nuc}$ in EGF signaling has yet to be defined. We show that in response to EGF, a GAL4 DNA-binding domain/carboxyl terminus Elk-1 chimera was inhibited in its ability to direct transcription from
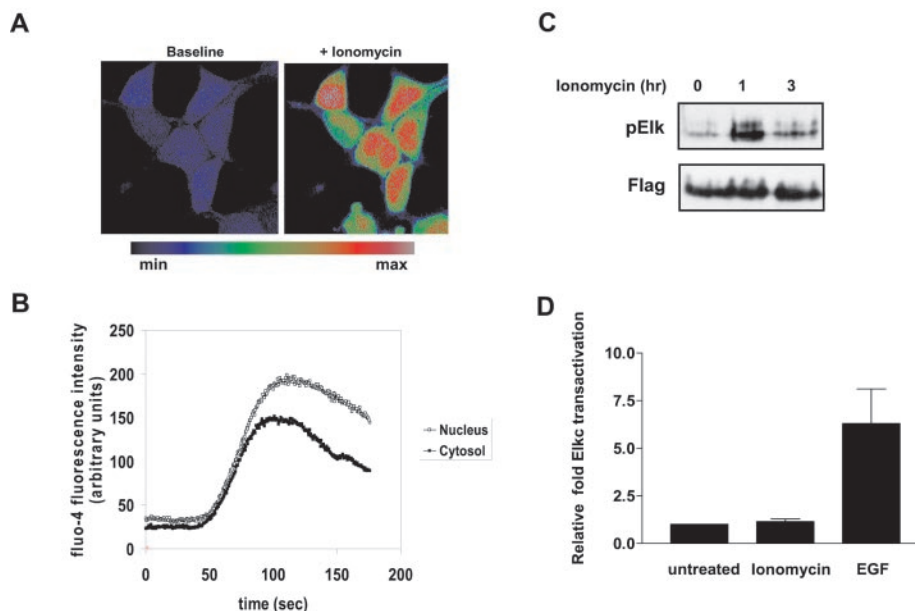
FIG. 11. **Uncoupling of Elk-1 phosphorylation from Elk-1 transactivation.** *A* and *B*, ionomycin induces Ca^{2+} signals in both the nucleus and cytosol of 293 cells. 293 cells loaded with fluo-4 were stimulated with 0.25 μM ionomycin and Ca^{2+} in both the nuclear and cytosolic compartment were monitored by confocal microscopy. Pseudocolor images of changes in Ca$^{2+}_{nuc}$ and Ca$^{2+}_{cyt}$ in 293 cells during stimulation with ionomycin are shown in *A*. The time course of changes in Ca$^{2+}_{nuc}$ and Ca$^{2+}_{cyt}$ in a representative 293 cell during stimulation with ionomycin is shown in *B*. *C*, 293 cells were treated with ionomycin (0.25 μM), and at the indicated times lysates were prepared and separated by SDS-PAGE. The proteins were transferred to Immobilon P membranes and immunoblotted with anti-phospho-Elk-1 antibodies. As a control this membrane was reprobed using anti-FLAG antibodies to detect for the expression of FLAG-Elk-1. *D*, 293 cells were transfected with Elk-1, 5XGAL4 luciferase, and β-galactosidase. Following serum starvation, 293 cells were left unstimulated or were stimulated with either ionomycin (0.25 μM) or EGF (10 ng/ml) for 5 h. Luciferase activities were normalized to β-galactosidase. These data represent the means $\pm$ S.E. of three separate experiments performed in triplicate.

a heterologous GAL4 DNA-binding element when PV was targeted to the nucleus. In contrast, expression of PV in the cytosol did not affect EGF-induced Elk-1 transactivation (Figs. 5 and 8). These data suggest that Ca$^{2+}_{nuc}$ but not Ca$^{2+}_{cyt}$ is involved in Elk-1-mediated regulation by EGF. However, this conclusion is predicated on the assumption that PV exerts its effects exclusively through buffering Ca^{2+}. We substantiated this in two ways. First, we demonstrated that EGF-mediated transactivation of Elk-1 was indeed Ca^{2+}-dependent through the use of the intracellular Ca^{2+} chelator BAPTA-AM (Fig. 4). Second, we generated a mutant within one of the two EF hands of PV, rendering PV deficient in its Ca^{2+} binding efficiency. When this PV mutant was expressed in the nucleus, at levels equivalent to that of the wild-type form of PV, EGF retained its ability to transactivate Elk-1 (Fig. 8). Thus, our findings provide strong evidence that the inhibitory effect of PV on EGF-induced Elk-1 transactivation is a direct consequence of the ability of PV to buffer Ca$^{2+}_{nuc}$. These data furthermore provide evidence for the specificity of PV as a tool for buffering Ca^{2+} and are the first to implicate the possibility that Ca$^{2+}_{nuc}$ signals participate in EGF-mediated transcriptional regulation.

The activation of Elk-1 is dependent upon phosphorylation within its carboxyl terminus at several residues by members of the MAPK family, including the ERKs (24, 33). Phosphorylation of Elk-1 then enhances its DNA binding through the serum response element, thereby promoting transcription (88). To provide a mechanistic basis for our finding that Ca$^{2+}_{nuc}$ is required for EGF-induced Elk-1 transactivation, we examined the effects of EGF on ERK activation in 293 cells expressing PV in the nucleus or cytosol. Interestingly, expression of PV in the nucleus of 293 cells failed to suppress EGF-induced ERK activation. The ability of ERK to translocate to the nucleus also was unaffected by expression of PV in the nucleus (Fig. 9). These data suggested that the inability of EGF to induce maximal Elk-1 transactivation is independent of ERK. Several

reports have described ERK-independent mechanisms for Elk-1 regulation (89–91); therefore we directly assessed the phosphorylation status of Elk-1. Surprisingly, Elk-1 was phosphorylated and localized to the nucleus following EGF stimulation, regardless of whether cells expressed PV in the nucleus. Thus, our data have identified that Elk-1 phosphorylation, specifically at Ser[383], can be dissociated from its transactivation following EGF stimulation. Additional evidence that this dissociation can occur was obtained by demonstrating that ionomycin also was able to phosphorylate Elk-1, without inducing Elk-1 transactivation. Collectively, these data suggest that Ca$^{2+}_{nuc}$ and Elk-1 phosphorylation both are necessary but not sufficient to mediate Elk-1 transcriptional activation by EGF. It is possible that EGF provides an additional signal not provided for by ionomycin that also is essential to initiate Elk-1 transactivation. It is important to note that our studies using this Elk-1-GAL4 chimera may not necessarily reflect the behavior of the native Elk-1 transcription factor in context with its cognate serum response element. Several studies have provided evidence to support the idea that phosphorylation of the transcriptional activation domain induces critical conformational changes in Elk-1 that regulate its transcriptional activity (88). Although transcription factors are modular in their structure, the effects of phosphorylation of Elk-1 may not be faithfully reflected in the Elk-1-GAL4 chimera used in these experiments. On the other hand, it is also reasonable to propose that additional EGF-regulated and Ca^{2+}-dependent co-factors interact with Elk-1 to induce maximal transcriptional activation.

The complexity of the EGF-Elk-1 signaling pathway is compounded by the fact that multiple signaling pathways converge on Elk-1. For example, Elk-1 is positively regulated by Ca^{2+} via the MAPKs and CaM-KII/IV pathways and negatively regulated by calcineurin (42, 44, 45). Thus, Elk-1 may be regulated directly via these Ca^{2+}-dependent kinases and phosphatases,

each of which has been found in the nucleus. It is likely that the balance among these opposing pathways will likely set the net state of Elk-1 responsiveness. Several reports have described MAPK-dependent and -independent pathways for the regulation of Elk-1 (24, 62, 89–91). Finally, it has also been suggested that both the kinetics and magnitude of the Ca^{2+} signal might be involved in the control of gene expression (10–12). Nuclear expression of PV may perturb these more subtle kinetic regulatory events of Ca^{2+} that ultimately could lead to attenuation of EGF-induced Elk-1 transactivation.

Our report describes a powerful tool in which to perturb Ca^{2+} signals distinctly within the nucleus and cytosol. This approach is amenable to the application of standard biochemical approaches, which has allowed us to reveal new insights into the role of nuclear Ca^{2+} in EGF-mediated regulation of Elk-1. Although we found that Ca$^{2+}_{nuc}$ is necessary for transactivation of Elk-1, additional work will be needed to determine how Ca$^{2+}_{nuc}$ links Elk-1 phosphorylation to its transactivation.

REFERENCES

1. Berridge, M. J. (1993) *Nature* **361,** 315–325
2. Clapham, D. E. (1995) *Cell* **80,** 259–268
3. Gomez, T. M., and Spitzer, N. C. (1999) *Nature* **397,** 350–355
4. Ito, K., Miyashita, Y., and Kasai, H. (1997) *EMBO J.* **16,** 242–251
5. Shen, S. S. (1995) *Curr. Top. Dev. Biol.* **30,** 63–101
6. Szalai, G., Krishnamurthy, R., and Hajnoczky, G. (1999) *EMBO J.* **18,** 6349–6361
7. Santella, L. (1998) *Biochem. Biophys. Res. Commun.* **244,** 317–324
8. Berridge, M. J., Bootman, M. D., and Lipp, P. (1998) *Nature* **395,** 645–648
9. Webb, S. E., and Miller, A. L. (2000) *Bioessays* **22,** 113–123
10. Li, W., Llopis, J., Whitney, M., Zlokarnik, G., and Tsien, R. Y. (1998) *Nature* **392,** 936–941
11. Dolmetsch, R. E., Xu, K., and Lewis, R. S. (1998) *Nature* **392,** 933–936
12. Dolmetsch, R. E., Lewis, R. S., Goodnow, C. C., and Healy, J. I. (1997) *Nature* **386,** 855–858
13. Zheng, J. Q. (2000) *Nature* **403,** 89–93
14. Ginty, D. D. (1997) *Neuron* **18,** 183–186
15. Johenning, F. W., Zochowski, M., Conway, S. J., Holmes, A. B., Koulen, P., and Ehrlich, B. E. (2002) *J. Neurosci.* **22,** 5344–5353
16. Humbert, J. P., Matter, N., Artault, J. C., Koppler, P., and Malviya, A. N. (1996) *J. Biol. Chem.* **271,** 478–485
17. Gerasimenko, O. V., Gerasimenko, J. V., Tepikin, A. V., and Petersen, O. H. (1995) *Cell* **80,** 439–444
18. Divecha, N., Banfic, H., and Irvine, R. F. (1991) *EMBO J.* **10,** 3207–3214
19. Lanini, L., Bachs, O., and Carafoli, E. (1992) *J. Biol. Chem.* **267,** 11548–11552
20. Nicotera, P., McConkey, D. J., Jones, D. P., and Orrenius, S. (1989) *Proc. Natl. Acad. Sci. U. S. A.* **86,** 453–457
21. Hardingham, G. E., Chawla, S., Johnson, C. M., and Bading, H. (1997) *Nature* **385,** 260–265
22. Chawla, S., Hardingham, G. E., Quinn, D. R., and Bading, H. (1998) *Science* **281,** 1505–1509
23. Sharrocks, A. D. (2001) *Nat. Rev. Mol. Cell. Biol.* **2,** 827–837
24. Treisman, R. (1996) *Curr. Opin. Cell Biol.* **8,** 205–215
25. Khokhlatchev, A. V., Canagarajah, B., Wilsbacher, J., Robinson, M., Atkinson, M., Goldsmith, E., and Cobb, M. H. (1998) *Cell* **93,** 605–615
26. Cobb, M. H. (1999) *Prog. Biophys. Mol. Biol.* **71,** 479–500
27. Davis, R. J. (1993) *J. Biol. Chem.* **268,** 14553–14556
28. Ip, Y. T., and Davis, R. J. (1998) *Curr. Opin. Cell Biol.* **10,** 205–219
29. Xia, Z., Dickens, M., Raingeaud, J., Davis, R. J., and Greenberg, M. E. (1995) *Science* **270,** 1326–1331
30. Chen, R. H., Sarnecki, C., and Blenis, J. (1992) *Mol. Cell. Biol.* **12,** 915–927
31. Yordy, J. S., and Muise-Helmericks, R. C. (2000) *Oncogene* **19,** 6503–6513
32. Marais, R., Wynne, J., and Treisman, R. (1993) *Cell* **73,** 381–393
33. Treisman, R. (1994) *Curr. Opin. Genet. Dev.* **4,** 96–101
34. Kamat, A., and Carpenter, G. (1997) *Cytokine Growth Factor Rev.* **8,** 109–117
35. Nojiri, S., and Hoek, J. B. (2000) *Hepatology* **32,** 947–957
36. Hepler, J. R., Nakahata, N., Lovenberg, T. W., DiGuiseppi, J., Herman, B., Earp, H. S., and Harden, T. K. (1987) *J. Biol. Chem.* **262,** 2951–2956
37. Maloney, J. A., Tsygankova, O. M., Yang, L., Li, Q., Szot, A., Baysal, K., and Williamson, J. R. (1999) *Am. J. Physiol.* **276,** C221–C230
38. Lev, S., Moreno, H., Martinez, R., Canoll, P., Peles, E., Musacchio, J. M., Plowman, G. D., Rudy, B., and Schlessinger, J. (1995) *Nature* **376,** 737–745
39. Anborgh, P. H., Qian, X., Papageorge, A. G., Vass, W. C., DeClue, J. E., and Lowy, D. R. (1999) *Mol. Cell. Biol.* **19,** 4611–4622
40. Means, A. R. (2000) *Mol. Endocrinol.* **14,** 4–13
41. Bernal-Mizrachi, E., Wen, W., Srinivasan, S., Klenk, A., Cohen, D., and Permutt, M. A. (2001) *Am. J. Physiol.* **281,** E1286–E1299
42. Enslen, H., Tokumitsu, H., Stork, P. J., Davis, R. J., and Soderling, T. R. (1996) *Proc. Natl. Acad. Sci. U. S. A.* **93,** 10803–10808
43. Cruzalegui, F. H., and Bading, H. (2000) *Cell. Mol. Life Sci.* **57,** 402–410
44. Sugimoto, T., Stewart, S., and Guan, K. L. (1997) *J. Biol. Chem.* **272,** 29415–29418
45. Tian, J., and Karin, M. (1999) *J. Biol. Chem.* **274,** 15173–15180
46. Fukuda, M., Gotoh, I., Adachi, M., Gotoh, Y., and Nishida, E. (1997) *J. Biol. Chem.* **272,** 32642–32648
47. Adachi, M., Fukuda, M., and Nishida, E. (2000) *J. Cell Biol.* **148,** 849–856
48. Pauls, T. L., Durussel, I., Cox, J. A., Clark, I. D., Szabo, A. G., Gagne, S. M., Sykes, B. D., and Berchtold, M. W. (1993) *J. Biol. Chem.* **268,** 20897–20903
49. Leite, M. F., Burgstahler, A. D., and Nathanson, M. H. (2002) *Gastroenterology* **122,** 415–427
50. Grynkiewicz, G., Poenie, M., and Tsien, R. Y. (1985) *J. Biol. Chem.* **260,** 3440–3450
51. Xu, C., Zipfel, W., Shear, J. B., Williams, R. M., and Webb, W. W. (1996) *Proc. Natl. Acad. Sci. U. S. A.* **93,** 10763–10768
52. Schlosser, S. F., Burgstahler, A. D., and Nathanson, M. H. (1996) *Proc. Natl. Acad. Sci. U. S. A.* **93,** 9948–9953
53. Minta, A., Kao, J. P., and Tsien, R. Y. (1989) *J. Biol. Chem.* **264,** 8171–8178
54. Andressen, C., Gotzos, V., Berchtold, M. W., Pauls, T. L., Schwaller, B., Fellay, B., and Celio, M. R. (1995) *Exp. Cell Res.* **219,** 420–426
55. Rasmussen, C. D., and Means, A. R. (1989) *Mol. Endocrinol.* **3,** 588–596
56. Fischer-Fantuizz, L., and Vesco, C. (1988) *Mol. Cell. Biol.* **8,** 5495–5503
57. Dubyak, G. R., and el-Moatassim, C. (1993) *Am. J. Physiol.* **265,** C577–C606
58. Burnstock, G. (1997) *Neuropharmacology* **36,** 1127–1139
59. Tanaka, Y., Hayashi, N., Kaneko, A., Ito, T., Miyoshi, E., Sasaki, Y., Fusamoto, H., and Kamada, T. (1992) *Hepatology* **16,** 479–486
60. Himpens, B., De Smedt, H., and Casteels, R. (1993) *Am. J. Physiol.* **265,** C966–C975
61. Pauls, T. L., Durussel, I., Berchtold, M. W., and Cox, J. A. (1994) *Biochemistry* **33,** 10393–10400
62. Fukuda, K., Tsuchihara, K., Hijikata, M., Nishiguchi, S., Kuroki, T., and Shimotohno, K. (2001) *Hepatology* **33,** 159–165
63. Santella, L., and Carafoli, E. (1997) *FASEB J.* **11,** 1091–1109
64. Malviya, A. N., and Rogue, P. J. (1998) *Cell* **92,** 17–23
65. Santella, L., and Kyozuka, K. (1997) *Cell Calcium* **22,** 11–20
66. Hennager, D. J., Welsh, M. J., and DeLisle, S. (1995) *J. Biol. Chem.* **270,** 4959–4962
67. Nicotera, P., and Rossi, A. D. (1994) *Mol. Cell. Biochem.* **135,** 89–98
68. Stehno-Bittel, L., Perez-Terzic, C., and Clapham, D. E. (1995) *Science* **270,** 1835–1838
69. Lee, M. A., Dunn, R. C., Clapham, D. E., and Stehno-Bittel, L. (1998) *Cell Calcium* **23,** 91–101
70. Heizmann, C. W. (1984) *Experientia* **40,** 910–921
71. Pauls, T. L., Cox, J. A., and Berchtold, M. W. (1996) *Biochim. Biophys. Acta* **1306,** 39–54
72. Kretsinger, R. H. (1980) *CRC Crit. Rev. Biochem.* **8,** 119–174
73. Berchtold, M. W. (1989) *Biochim. Biophys. Acta* **1009,** 201–215
74. Celio, M. R. (1986) *Science* **231,** 995–997
75. Schneeberger, P. R., and Heizmann, C. W. (1986) *FEBS Lett.* **201,** 51–56
76. Kagi, U., Berchtold, M. W., and Heizmann, C. W. (1987) *J. Biol. Chem.* **262,** 7314–7320
77. Endo, T., Takazawa, K., and Onaya, T. (1985) *Endocrinology* **117,** 527–531
78. Muntener, M., Kaser, L., Weber, J., and Berchtold, M. W. (1995) *Proc. Natl. Acad. Sci. U. S. A.* **92,** 6504–6508
79. Wahr, P. A., Michele, D. E., and Metzger, J. M. (1999) *Proc. Natl. Acad. Sci. U. S. A.* **96,** 11982–11985
80. Szatkowski, M. L., Westfall, M. V., Gomez, C. A., Wahr, P. A., Michele, D. E., DelloRusso, C., Turner, I., Hong, K. E., Albayya, F. P., and Metzger, J. M. (2001) *J. Clin. Invest.* **107,** 191–198
81. Caillard, O., Moreno, H., Schwaller, B., Llano, I., Celio, M. R., and Marty, A. (2000) *Proc. Natl. Acad. Sci. U. S. A.* **97,** 13372–13377
82. Loza, J., Marzec, N., Simasko, S., and Dziak, R. (1995) *Cell Calcium* **17,** 301–306
83. Magni, M., Meldolesi, J., and Pandiella, A. (1991) *J. Biol. Chem.* **266,** 6329–6335
84. Hill, T. D., Kindmark, H., and Boynton, A. L. (1988) *J. Cell. Biochem.* **38,** 137–144
85. Ichikawa, J., and Kiyohara, T. (2001) *Cell Biochem. Funct.* **19,** 213–219
86. Wagstaff, S. C., Bowler, W. B., Gallagher, J. A., and Hipskind, R. A. (2000) *Carcinogenesis* **21,** 2175–2181
87. Lenormand, P., Pribnow, D., Rodland, K. D., and Magun, B. E. (1992) *Mol. Cell. Biol.* **12,** 2793–2803
88. Yang, S. H., Shore, P., Willingham, N., Lakey, J. H., and Sharrocks, A. D. (1999) *EMBO J.* **18,** 5666–5674
89. Gu, H., Pratt, J. C., Burakoff, S. J., and Neel, B. G. (1998) *Mol. Cell* **2,** 729–740
90. Zhao, C., Yu, D. H., Shen, R., and Feng, G. S. (1999) *J. Biol. Chem.* **274,** 19649–19654
91. Sugimoto, T., Stewart, S., Han, M., and Guan, K. L. (1998) *EMBO J.* **17,** 1717–1727